Substrate influence on the plasmonic response of clusters of spherical nanoparticles

P. A. Letnes* and I. Simonsen
Department of Physics, The Norwegian University of Science and Technology (NTNU), NO-7491 Trondheim, Norway

D. L. Mills
Department of Physics and Astronomy, University of California, Irvine, California 92697, USA
(Received 16 November 2010; published 23 February 2011)

The plasmonic response of nanoparticles is exploited in many subfields of science and engineering to enhance optical signals associated with probes of nanoscale and subnanoscale entities. We develop a numerical algorithm based on previous theoretical work that addresses the influence of a substrate on the plasmonic response of collections of nanoparticles of spherical shape. Our method is a real-space approach within the quasistatic limit that can be applied to a wide range of structures. We illustrate the role of the substrate through numerical calculations that explore single nanospheres and nanosphere dimers fabricated from either a Drude model metal or from silver on dielectric substrates and from dielectric spheres on silver substrates.

DOI: 10.1103/PhysRevB.83.075426 PACS number(s): 78.67.Bf

I. INTRODUCTION

Currently there is great interest in the use of the plasmonic response of tailored metallic substrates and other structures for the purpose of enhancing electric fields of laser beams in their near vicinity. Enhancements with an origin in the excitation of collective plasmon modes can increase the field intensity by many orders of magnitude in the near vicinity of diverse systems. This phenomenon was first explored in the context of surface-enhanced Raman scattering (SERS), wherein it was found that the Raman cross section of pyridine adsorbed on electrochemically roughened Ag surfaces can be enhanced by approximately 6 orders of magnitude relative to that realized for pyridine in solution.[1] The field has evolved to the point where the Raman spectrum of single molecules can be detected through the use of plasmon-enhanced Raman probes.[2,3] Plasmonic enhancements can be used not only in the context of Raman spectroscopy, but also, more generally, to enhance the cross section of diverse nonlinear optical processes.[4,5]

In the theoretical literature, one finds numerous studies of the plasmonic response of isolated nanoparticles of diverse shape[6,7] along with metallic arrays of nanoparticles.[8,9] So far as we know, virtually all such discussions explore nanoparticles and their arrays in free space.[10,11] Treatments of the free-space response are appropriate for clusters of nanoparticles in solution, but commonly, one is interested in particles and particle arrays on substrates. Then, an issue is the influence of the nanoparticle-substrate interaction on the plasmonic response of the nanoparticles that reside on it. Papers addressing particle-substrate interactions include the work of Yamaguchi *et al.*,[12] which discussed particles above substrates in the dipole approximation. Work done by Ruppin[13] and by Román-Velázquez *et al.*[14] and Noguez[15] also deal with sphere-substrate interactions but only for a single nanoparticle. Mayergoyz *et al.* have studied the plasmon eigenfrequencies of nanosphere dimers and also cylindrical structures on a substrate.[7] Moreover, a recent study on the plasmonic response of cubical nanoparticle dimers[16] reports on the dimer-substrate interactions in the SERS context.

Since the early 1970s, Bedeaux and Vlieger have conducted numerous theoretical and numerical studies on the effects of particle-substrate and particle-particle interactions.[17] These studies have been concentrated around spherical or spheroidal particles on top of a substrate or *truncated* particles of such shapes on a substrate (used to model a finite contact angle). In a paper based on the formalism of Bedeaux and Vlieger, the particle-substrate interactions were taken into account to high multipolar order, while the particle-particle interactions were only calculated to dipolar or quadrupolar order, since their main concern was systems where the particle coverage is low.[18]

More recently, numerical studies based on Bedeaux and Vlieger's work have been carried out by Lazzari and coworkers for the purpose of *in situ* inversion of experimental optical spectra obtained from growing thin granular metal films.[18–21]

In this paper, we present a description of the influence of a substrate on the plasmonic response of nonperiodic nanosphere arrays; through the use of the Bloch theorem, one may address periodic systems as well. We employ the quasistatic description of the response of the system. This proves adequate for objects whose linear dimensions are small compared to the wavelength of light.[22] In contrast to previous work, we consistently take into account higher-order interactions between the nanospheres.

After we describe the formalism, we turn our attention to calculations that explore the influence of the substrate on the response of nanospheres and nanosphere dimers. Of interest is the discussion of hot-spot regions where, at selected excitation frequencies, one realizes very large field enhancements by virtue of the excitation of collective plasmon modes. For the case of two spheres in free space that are nearly in contact, one realizes a hot spot at the point of closest contact between the spheres.[23,24] In this paper, for a nanosphere dimer near a dielectric substrate, we find moving hot spots. A small change in excitation frequency can cause the hot spot to move from the point of nearest contact between the spheres to the south poles of the spheres—the points on the spheres closest to the substrate. In recent work, two of the authors have discussed moving hot spots in nanosphere clusters.[25]

This paper illustrates the role of the substrate in creating new hot spots. We find that, if a dielectric sphere is in close proximity to a plasmonic active metallic substrate, the region

around the south pole of the dielectric sphere becomes a hot spot. A spatially localized potential well that can trap substrate plasmons is formed just under the dielectric sphere. Also, if a metallic sphere is placed close to a dielectric substrate, we find a collective plasmon localized near the south pole of the sphere. Thus, the interaction of nanospheres and structured arrays of such objects placed on substrates creates new hot spots that can be exploited in diverse nonlinear optical spectral probes of nanoscale and subnanoscale matter.

In this paper, Sec. II is devoted to setting up a formalism that may be applied to any nonperiodic structure of spherical nanoparticles that are located on, or near, a substrate, and Sec. III presents the results of our numerical studies of isolated nanospheres and nanosphere dimers on substrates. Section IV contains concluding remarks.

II. THEORY

Even if the numerical calculations to be performed in this paper will focus on one or two nanoparticles, we will, however, present a more general formalism valid for a cluster of N nanoparticles. For the case of the dimer, the geometry is illustrated in Fig. 1. The substrate is located in the half space $z < 0$, and it is characterized by the dielectric function $\varepsilon_-(\omega)$. The region above the substrate, $z > 0$, is assumed to be a nonabsorbing dielectric characterized by the dielectric function $\varepsilon_+(\omega)$.

We consider a system consisting of N nonoverlapping nanospheres, located at arbitrary positions. For each such sphere, we embed a coordinate system $\mathcal{S}_j$, $j = 1,2,\ldots N$ so that the origin of $\mathcal{S}_j$ is located at the center of sphere j. With each coordinate system $\mathcal{S}_j$, we associate a position vector $\boldsymbol{r}_j = (r_j,\theta_j,\phi_j)$.

Our interest is in nanosphere arrays whose extent is small compared to the wavelength of light, so the electrostatic approximation suffices to describe the electric fields in its vicinity. Under this assumption, the Maxwell equations are equivalent to the Laplace equation. Thus, our task is to solve Laplace's equation for the electrostatic potential ψ,

$$\nabla^2\psi = 0,$$

subject to the appropriate boundary conditions on the surface of each sphere and at the interface between the substrate and the rest of the system. As usual, the electric field is given by[22] $\boldsymbol{E} = -\boldsymbol{\nabla}\psi$.

We will assume that a spatially uniform electric field $\boldsymbol{E}_0$ of angular frequency ω is applied to the system, and we analyze its response to this field. In what follows, all dielectric functions that enter the analysis are the complex dielectric functions appropriate for the frequency ω, although we suppress any explicit reference to ω in what follows. Hence, the electrostatic potential in the half space $z > 0$ can be written as

$$\psi_+(\boldsymbol{r}) = -\boldsymbol{r}\cdot\boldsymbol{E}_0 + \sum_{j=1}^{N}\psi_j(\boldsymbol{r}_j) + \sum_{\bar{j}=1}^{N}\psi_{\bar{j}}(\boldsymbol{r}_{\bar{j}}), \tag{1}$$

where ψ_j is the electrostatic potential produced by the polarization charges in sphere j and $\psi_{\bar{j}}$ is the potential produced by its image, located in the half space $z < 0$. In the substrate ($z < 0$), the electrostatic potential takes the form

$$\psi_-(\boldsymbol{r}) = -\boldsymbol{r}\cdot\boldsymbol{E}_0^T + \sum_{j=1}^{N}\psi_j^T(\boldsymbol{r}_j), \tag{2}$$

where ψ_j^T is the electrostatic potential of sphere j as seen by an observer in the region $z < 0$, and $\boldsymbol{E}_0^T$ is the applied field in the substrate. The various single-sphere potential functions that enter Eqs. (1) and (2) may be expanded in the spherical harmonics. Using the shorthand notation $\sum_{lm} = \sum_{l=0}^{\infty}\sum_{m=-l}^{l}$, we have

$$\psi_j(\boldsymbol{r}_j) = \begin{cases} \sum_{lm} A_{lm}^{(j)} r_j^{-l-1} Y_l^m(\theta_j,\phi_j), & r_j \geqslant a_j, \\ \sum_{lm} B_{lm}^{(j)} r_j^{l} Y_l^m(\theta_j,\phi_j), & r_j < a_j, \end{cases} \tag{3a}$$

$$\psi_{\bar{j}}(\boldsymbol{r}_{\bar{j}}) = \sum_{lm} A_{lm}^{(j,R)} r_{\bar{j}}^{-l-1} Y_l^m(\theta_{\bar{j}},\phi_{\bar{j}}), \tag{3b}$$

and

$$\psi_j^T(\boldsymbol{r}_j) = \textstyle\sum_{lm} A_{lm}^{(j,T)} r_j^{-l-1} Y_l^m(\theta_j,\phi_j), \tag{3c}$$

where the various A_{lm} and B_{lm} are expansion coefficients to be determined and a_j refers to the radius of sphere j. The symbol Y_l^m refers to the spherical harmonic functions as described in Ref. 22. As discussed in Refs. 17 and 19, the coefficients $A_{lm}^{(j,R)}$ and $A_{lm}^{(j,T)}$ are related to $A_{lm}^{(j)}$ through the boundary conditions at the interface $z = 0$. Simple image arguments supply the relation between these quantities. In particular, one finds that[17,19]

$$A_{lm}^{(j,R)} = (-1)^{l+m}\frac{\varepsilon_+ - \varepsilon_-}{\varepsilon_+ + \varepsilon_-} A_{lm}^{(j)}, \tag{4a}$$

and

$$A_{lm}^{(j,T)} = \frac{2\varepsilon_+}{\varepsilon_+ + \varepsilon_-} A_{lm}^{(j)}. \tag{4b}$$

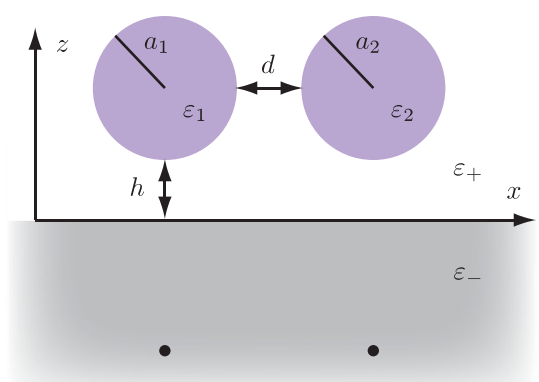

FIG. 1. (Color online) An illustration of the system we consider in this paper, for the case where we have a nanosphere dimer. The substrate occupies the half space $z < 0$, h is the distance between the south poles of the spheres and the substrate, and d is their surface-surface separation. Sphere j of the dimer has dielectric function $\varepsilon_j(\omega)$ and radius a_j. The medium above the substrate has dielectric function $\varepsilon_+(\omega)$ while that of the substrate is $\varepsilon_-(\omega)$. The two black dots schematically represent image multipoles in the substrate seen by an observer in the half space $z > 0$.

Equation (4) ensures that the boundary conditions on the substrate ($z = 0$) are automatically satisfied for any $A_{lm}^{(j)}$. Thus, in what follows, we seek to solve for the coefficients $A_{lm}^{(j)}$ and $B_{lm}^{(j)}$ using the equations that follow from the boundary conditions at the surface of each nanosphere, i.e., where $r_j = a_j$. Through rearrangement of the equations following from the boundary conditions on the sphere surfaces, one can eliminate the coefficients $B_{lm}^{(j)}$. In the Appendix, the linear set of equations determining $A_{lm}^{(j)}$ and $B_{lm}^{(j)}$ are derived [cf. Eq. (A4)].

In Sec. III, we present a series of numerical studies of plasmon resonance phenomena for nanosphere monomers and dimers placed on a substrate. To this end, we must solve Eq. (A4). In order to do so, we truncate the summations in Eq. (3) and also the equation system in Eq. (A4) at $l = L$. The number of unknown coefficients in Eq. (A4) is then $N(L+1)^2 - 1$. We use the same truncation limit for both the nanosphere-nanosphere interactions as well as for the nanosphere-substrate interactions. The nanosphere-substrate interactions include both the interaction of a given nanosphere with its own image and the images of the other nanospheres. Note that all particle-substrate *and* particle-particle interactions consistently have been taken into account (to a given order). In several previous studies, the interaction with the substrate has been taken into account to a high order, while the particle-particle interactions have been accounted for at dipolar or quadrupolar order.[17–21] In Sec. III, we will see that the use of the dipole approximation (retention of only the terms with $l = 1$) in the particle-substrate interaction is very inaccurate from a quantitative point of view save for the case when the nanospheres are quite far from the substrate.

In passing, we note that the formalism presented in this paper can be applied to extend the formalism used in Ref. 9 to incorporate interactions of periodic structures with a substrate. One then has plasmon normal modes characterized by a wave vector $\boldsymbol{k}_\parallel$ parallel to the surface; one encounters only $(L+1)^2$ coefficients in this case because the expansion coefficients of different nanoparticles are linked by the Bloch theorem. The quasistatic limit developed in this paper can be applied to the description of collective excitations whose wave vector is large compared to ω/c with ω as the angular frequency of an excitation of interest and c as the velocity of light in vacuum.

III. RESULTS AND DISCUSSION

In this section, we present a series of studies of the influence of a dielectric substrate on the plasmonic response of isolated nanospheres and nanosphere dimers. In addition, we find hot spots created by plasmonic resonances between dielectric spheres and metallic substrates, as noted before. We will also see that termination of the hierarchy of equations at the dipole ($L = 1$, see Ref. 12) or quadrupole ($L = 2$) order provides a very poor quantitative description of interactions between particles and between the particles and the substrate. We remark that it is evident from earlier studies, which utilize a different methodology,[24] that higher-order harmonics must be included in the description of particle-particle interaction, since the fields associated with hot spots are highly localized around the points of nearest contact. Thus, one must retain spherical harmonics at high order to describe these features.

For the purpose of studying particle-substrate interactions, we first consider nanoparticles modeled by a dielectric function of the Drude form,[22]

$$\varepsilon(\omega) = 1 - \frac{\omega_P^2}{\omega(\omega + \mathrm{i}\gamma)}, \tag{5}$$

where ω_P is the plasma frequency and γ is the inverse of the free carrier relaxation time. For the ambient material, we have chosen vacuum, i.e., $\varepsilon_+ = 1$ and a dielectric substrate of $\varepsilon_- > 0$. The virtue of model studies based on the form of Eq. (5) is that we may choose the relaxation rate γ sufficiently small so that much detail is evident in the calculated results. For the Drude model parameters, we assume $\omega_P = 3$ eV and $\gamma = 0.03$ eV. After our discussion of nanospheres consisting of Drude metal, we present results for geometries incorporating silver (Ag) nanoparticles. Among metals that exhibit plasmonic response in the visible part of the optical spectrum, the damping rate in Ag is modest, and numerous experiments employ Ag-based structures.[26] It should be remarked that the optical response of aluminum (Al) is described very well by the Drude model. Unfortunately, the plasma frequency is very high, close to 15 eV, so the interesting plasmonic resonances in Al-based materials lie well into the ultraviolet. In our view, it would be of great interest to see experimental probes of structures that incorporate Al nanoparticles, with attention to the appropriate spectral range.

One possible indicator of plasmonic activity is the total dipole moment of one of our spherical objects. With $\boldsymbol{p}(\omega)$ being the dipole moment of a nanosphere at angular frequency ω, we define the dimensionless dipole moment as

$$\bar{\boldsymbol{p}} = \frac{\boldsymbol{p}}{a^3 \varepsilon_0 E_0},$$

where a is the radius of the sphere in question and ε_0 is the vacuum permeability. In terms of our expansion coefficients A_{lm}, the three Cartesian components of the dimensionless dipole moment are given by

$$\bar{p}_x = \sqrt{\frac{3}{8\pi}} \frac{A_{1,-1} - A_{1,1}}{a^2},$$

$$\bar{p}_y = -\mathrm{i}\sqrt{\frac{3}{8\pi}} \frac{A_{1,-1} + A_{1,1}}{a^2},$$

and

$$\bar{p}_z = \sqrt{\frac{3}{4\pi}} \frac{A_{10}}{a^2}.$$

Since the dipole moment in general is a complex vector quantity, the quantity we display in the figures that follow is the modulus of the total dipole moment given by

$$\bar{p}(\omega) \equiv |\bar{\boldsymbol{p}}(\omega)| = \sqrt{\bar{\boldsymbol{p}}^\dagger \bar{\boldsymbol{p}}},$$

where † symbolizes the Hermitian transpose. In our studies of the interaction of a single sphere with the substrate, we will display the total dimensionless dipole moment, along with field-enhancement factors for applied fields perpendicular to the substrate ($\boldsymbol{E}_0 \parallel \hat{\boldsymbol{z}}$) as well as parallel to the substrate ($\boldsymbol{E}_0 \parallel \hat{\boldsymbol{x}}$). Moreover, for the dimer illustrated in Fig. 1, we will present results for all three Cartesian components of the applied field.

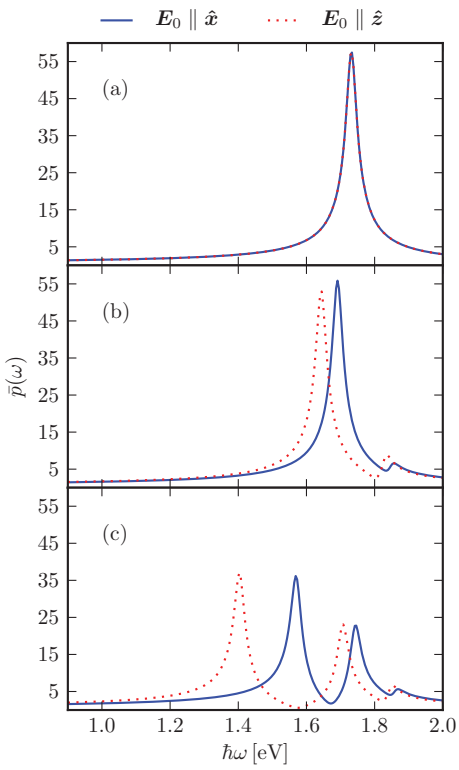

FIG. 2. (Color online) The dimensionless dipole moment $\bar{p}(\omega)$, for a Drude metal particle on a substrate of dielectric function (a) $\varepsilon_- = 1$, (b) $\varepsilon_- = 2$, and (c) $\varepsilon_- = 10$. For the vacuum case, i.e., $\varepsilon_- = 1$, we obtain the Mie result at $\hbar\omega = \hbar\omega_P/\sqrt{3} \approx 1.73$ eV. For all plots, we have $h = 0.05a$, $\omega_P = 3$ eV, $\gamma = 0.03$ eV, and $L = 50$.

A. The Drude monomer and dimer

We begin by considering a single Drude sphere in vacuum ($\varepsilon_+ = 1$) located a distance $h = 0.05a$ above a substrate. In Fig. 2, we present numerical calculations of the dimensionless dipole moment for three choices of the dielectric function of the substrate, $\varepsilon_- = 1$, 2, and 10. The choice $\varepsilon_- = 1$ corresponds physically to the case where no substrate is present. We present results for two choices of the applied field: (i) perpendicular to the substrate (z direction, red dotted curves) and (ii) parallel to the substrate (x direction, blue solid curves). Since the system is invariant with respect to rotation about the z axis, the response to an applied field parallel to the y axis is identical to that shown for x polarization.

In Fig. 2(a), we present the response of the sphere in free space, from which the Mie resonance at the frequency $\hbar\omega_P/\sqrt{3} \approx 1.73$ eV is readily observed. While an isolated Drude metal sphere has a spectrum of multipole modes at angular frequencies $\omega_l = \omega_P\,[l/(2l+1)]^{1/2}$ with $l = 1,2,3,\ldots$, only the dipole mode with $l = 1$ is excited by an applied field whose wavelength is large compared to the radius of the sphere. In the presence of a substrate, higher-order modes may be excited by a spatially uniform applied field, as we will see. These will appear at higher frequencies than the Mie resonance, as suggested by the fact that $\omega_{l+1} > \omega_l$ for $l \geqslant 1$.

When the dielectric function of the substrate is $\varepsilon_- > \varepsilon_+$, the spectral response of the nanosphere is altered significantly. First, for the case of modest dielectric function $\varepsilon_- = 2$, the (former) Mie resonance remains the dominant spectral feature, and it is redshifted by the proximity of the dielectric substrate to the nanosphere [Fig. 2(b)]. A substantial splitting of the modes is observed when the response to a field parallel to the substrate is compared to the response to a field perpendicular to it. We also see activation of a higher-frequency mode. One might be tempted to associate this with excitation of the quadrupolar mode with $l = 2$, but when the sphere is so close to the substrate, classification of the mode by the angular momentum quantum number is no longer accurate since a large number of l modes are mixed together. We require L, the cutoff used in the hierarchy of equations displayed in Eq. (A4), to be on the order of 30 (or more) to obtain converged results.

If the substrate has a large dielectric function ($\varepsilon_- = 10$), then the response of the sphere is modified dramatically relative to the free-space case [Fig. 2(c)]. The splitting of the low-frequency resonances, for parallel and perpendicular excitations, is now very large. For both orientations of the applied field, the oscillator strength of the next highest mode is comparable to the low-frequency (dipole) mode. We also see a third mode in the spectrum, so the symmetry breaking provided by the substrate now asserts itself prominently in the response of the sphere.

The appearance of these higher-order modes can be intuitively understood as follows. When we apply an electric field $\boldsymbol{E}_0$ to a nanosphere, it will generate local evanescent fields. When h is small, some of the evanescent fields are reflected from the substrate, resulting in a nonuniform field around the sphere. This causes the simultaneous excitation of many different l modes, meaning that the notion of discussing modes in multipolar terminology breaks down badly. The cross talk between different l modes is also the reason why we see higher-order modes (e.g., quadrupole modes) in the dipole moment [$\bar{p}(\omega)$] of the spheres.

We now turn our attention to a discussion of the response of a Drude dimer, as shown in Fig. 1. The radii of the two spheres are both assumed to be equal to a. The distance between the spheres is $d = 0.1a$, and they are both placed a distance $h = 0.05a$ above the substrate. In Fig. 3, we depict the dimensionless dipole moment of one of the spheres in a dimer whose axis is parallel to the x axis and, hence, to the substrate.

When the dimer is placed in free space [Fig. 3(a)] and the applied field is perpendicular to the dimer axis, there is one dominant resonance. This is the Mie resonance of the single sphere, slightly blueshifted due to the particle-particle interactions. In addition, a second weak mode shows up at higher frequencies. In contrast, when the dimer is excited by a field parallel to the dimer axis (blue solid curve), we see a sequence of collective modes redshifted by large amounts from the isolated sphere Mie resonance. These results are in agreement with previous work on nanoparticle dimers in free space.[24] As for the case of the single sphere on a substrate, the fields generated from one sphere cause higher-order modes to be excited in the other sphere, and vice versa.

For a substrate with modest dielectric function [$\varepsilon_- = 2$, Fig. 3(b)], we see a splitting between the dominant collective modes excited by a field parallel to $\hat{\boldsymbol{z}}$ (red dotted curve) and that excited by a field parallel to $\hat{\boldsymbol{y}}$ (green dashed curve). This is to be expected since the presence of the substrate will break

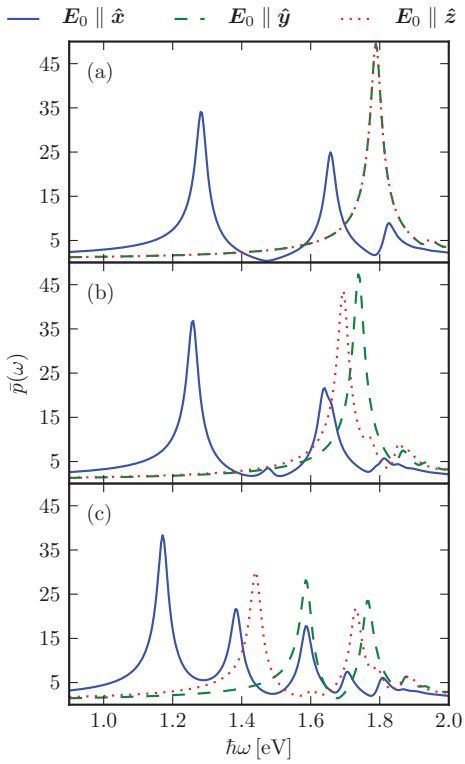

FIG. 3. (Color online) The dimensionless dipole moment $\bar{p}(\omega)$, for one of the particles in a Drude metal dimer, on top of a substrate of dielectric function (a) $\varepsilon_- = 1$, (b) $\varepsilon_- = 2$, and (c) $\varepsilon_- = 10$. For all plots, we have $h = 0.05a$, $d = 0.1a$, $\omega_P = 3$ eV, $\gamma = 0.03$ eV, and $L = 50$.

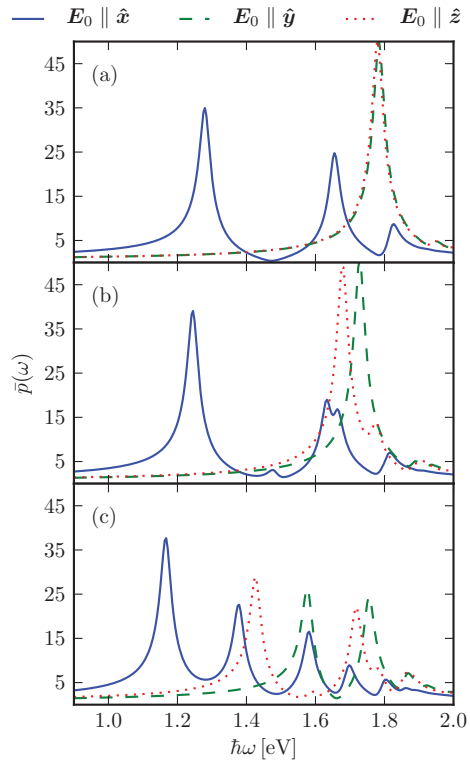

FIG. 4. (Color online) The plots show $\bar{p}(\omega)$ for one of the particles in a Drude metal dimer for (a) $h = 2a$, (b) $h = 0.3a$, and (c) $h = 0.05a$. For all plots, we have $\varepsilon_- = 10$, $d = 0.1a$, $\omega_P = 3$ eV, $\gamma = 0.03$ eV, and $L = 30$.

the rotational symmetry around the x axis. If the dielectric function of the substrate is substantial [$\varepsilon_- = 10$, Fig. 3(c)], we observe dramatic differences between the spectral response for the three directions of the applied field. The shift of the lowest-frequency mode for $\boldsymbol{E}_0 \parallel \hat{\boldsymbol{x}}$ from the Mie resonance of the isolated sphere is particularly dramatic.

These results demonstrate that placing metallic nanosphere dimers over a substrate with a large dielectric function will give rise to substantial field enhancements. Also, strong dipole moment enhancements can be achieved over a very large spectral range compared to that realized for a single isolated nanosphere. Thus, as this example illustrates, the interaction between structured nanoparticle arrays and a substrate of substantial dielectric function can allow one to design objects with a broad plasmonic spectral response.

Figure 4 shows how the response of the dimer depends on the distance h above the substrate. A substrate dielectric function $\varepsilon_- = 10$ was assumed in order to emphasize the influence of the substrate on the response of the dimer. In Fig. 4(a), where $h = 2a$, the spectral response is very close to that of the isolated dimer, shown in Fig. 3(a). We see clear interaction effects with the substrate when $h = 0.3a$ [Fig. 4(b)], but it remains true that the spectrum is qualitatively similar to that of the free dimer. The dimer has to be close to the substrate for the interaction effects to modify the spectrum even for the large substrate dielectric function used in these calculations [Fig. 4(c)].

We pause for a moment to comment on issues of convergence. It is common to employ the dipole approximation to describe intersphere interactions and interactions of nanoparticles with substrates using the image method.[12] In Fig. 5, we present how the position of the lowest-energy collective mode for the case $\boldsymbol{E}_0 \parallel \hat{\boldsymbol{z}}$ depends on L, which determines the number of unknown A_{lm} coefficients in Eq. (A4). The frequently used dipole approximation corresponds to $L = 1$, and from Fig. 5, one observes that it is inaccurate even when the dimer is far above the substrate ($h = 2a$) and becomes gradually worse as h is decreased. The cutoff L must be on the order of 30 to obtain converged results for the parameter ranges explored in this paper. One may appreciate the reason for this from earlier work.[24] When two spheres are quite close to each other, one encounters collective modes wherein the fields are concentrated in a small angular range near the points of closest contact. Similarly, when one or more nanospheres are very close to a dielectric substrate, one encounters collective modes localized around the south pole of the spheres—the points closest to the substrate. One requires large values of the cutoff L if one wishes to describe such modes accurately. Notice, by the way, that the mode frequency is significantly redshifted when the dimer comes very close to touching the substrate. In passing, we note that convergent results do not guarantee correctness of the calculated potentials. In order to do so, one has to explicitly make sure that the boundary conditions are satisfied for the required accuracy at all points on all interfaces.[19]

In Fig. 6, we examine the nature of the enhanced fields in the Drude dimer at the two points indicated in the inset. Again, we

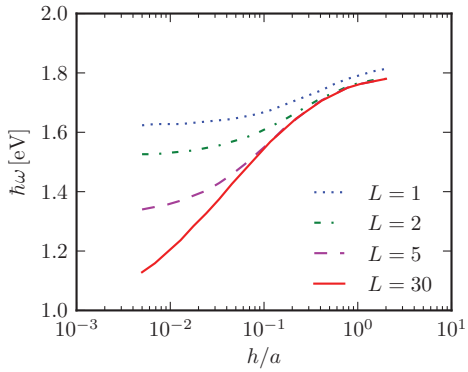

FIG. 5. (Color online) Position of the lowest-energy resonance as a function of h, in the case where $\boldsymbol{E}_0 \parallel \hat{\boldsymbol{z}}$. The blue dotted curve shows the result when the calculation is done in the dipole approximation (i.e., $L = 1$), while the red solid curve $L = 30$ shows the converged results. For all cases, a Drude dimer with $d = 0.1a$ was assumed, and the substrate dielectric function was $\varepsilon_- = 10$.

have assumed $d = 0.1a$ and $h = 0.05a$ in these calculations. For most of the spectrum, the largest field enhancement is found at point 2, the hot spot where the two spheres nearly touch. Notice, however, that we also have very large field enhancements between the south pole of the spheres and the dielectric substrate, in particular, at 1.35 eV [see Figs. 6 and 7(a)]. In our view, the region where the dielectric substrate is very close to the bottom of the sphere acts like an effective potential well that traps surface plasmons at the south pole. The surface plasmons sense the presence of the dielectric through the fields associated with them in the region outside the sphere.

From Fig. 6, we can see that points 1 and 2 are hot simultaneously at roughly the same frequency. However, as one scans through a given resonance peak, near $\hbar\omega = 1.4$ eV in Fig. 6, the hot spot moves from point 1 to point 2 and conversely, depending on the precise value of the frequency. Thus, we have another example of the phenomenon of the moving hot spots discussed in a recent publication.[25] We illustrate this behavior in Fig. 7, where we plot $|\boldsymbol{E}|/|\boldsymbol{E}_0|$ on a contour map.[27] A small energy shift of 0.1 eV is enough to

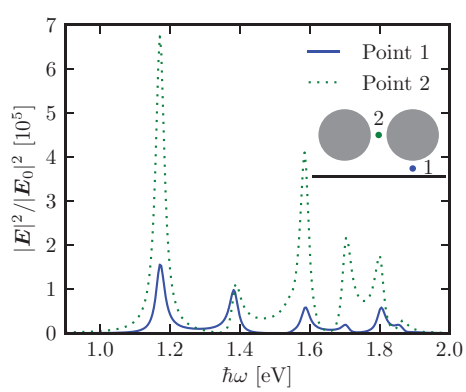

FIG. 6. (Color online) The square of the electric field $|\boldsymbol{E}|^2/|\boldsymbol{E}_0|^2$, at point 1 (blue solid curve) and point 2 (green dotted curve) as a function of frequency, for the Drude dimer. The results are for the case where $\boldsymbol{E}_0 \parallel \hat{\boldsymbol{x}}$, and the substrate dielectric function is $\varepsilon_- = 10$. The other parameters are the same as in Fig. 3.

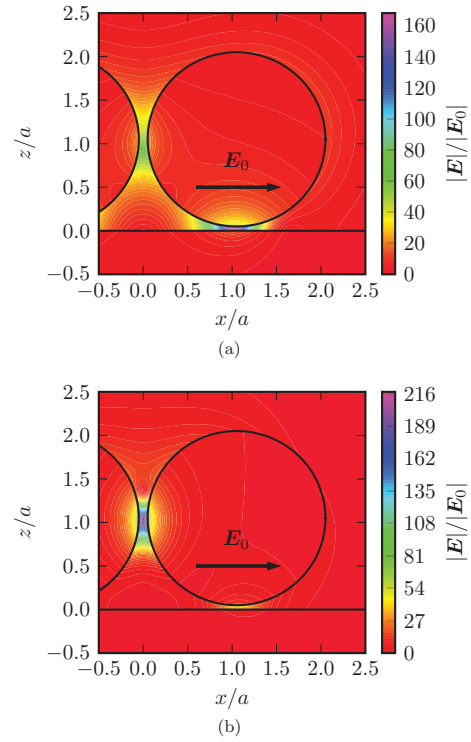

FIG. 7. (Color online) The field enhancement $|\boldsymbol{E}|/|\boldsymbol{E}_0|$ in the xz plane. At (a) $\hbar\omega = 1.35$ eV, the highest field enhancement is found between the sphere and the substrate; at (b) $\hbar\omega = 1.45$ eV, the highest field enhancement is found on the line connecting the two spheres. As shown in the figure, $\boldsymbol{E}_0 \parallel \hat{\boldsymbol{x}}$. The system parameters are $\varepsilon_- = 10$, $h = 0.05a$, $d = 0.1a$, and $L = 50$. Of particular interest is the area between the two lowest-frequency peaks, where the location of maximum field enhancement flips between the two points indicated.

change the shape of the field enhancement considerably and move the hot spot from point 1 to point 2.

B. Ag monomers and dimers

The Drude model discussed in Sec. III A is useful to examine, since one may model metals in which the plasmons are damped very lightly. Thus, one can explore detailed structure in the response of the model system. In practice, however, interest resides in realistic metals that display plasmonic response in the visible. In this respect, silver (Ag) and gold (Au) are the two metals most studied experimentally. While Au is indeed plasmon active, the plasmons in this material are, in fact, rather heavily damped. Ag is a much better material in principle, even though in experiments oxide can form on its surface.

This section is devoted to studies of the plasmon resonance properties of Ag monomers and dimers. Figure 8 shows calculations of the reduced dipole moment for a single Ag nanosphere placed a distance $h = 0.05a$ over a dielectric substrate. For a free-standing Ag sphere in vacuum, the Mie resonance at $\hbar\omega = 3.5$ eV is readily observed [Fig. 8(a)]. The response of the sphere is modest for $\varepsilon_- = 2$ [Fig. 8(b)]. However, when $\varepsilon_- = 10$ [Fig. 8(c)], we see a substantial splitting of the main resonance and activation of higher-frequency modes occur.

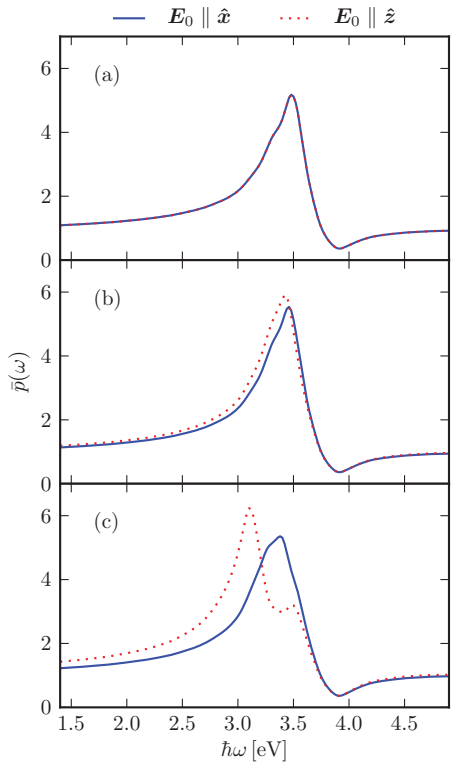

FIG. 8. (Color online) The dimensionless dipole moment for an Ag sphere placed a distance $h = 0.05a$ above a dielectric substrate of (a) $\varepsilon_- = 1$, (b) $\varepsilon_- = 2$, and (c) $\varepsilon_- = 10$. The equation system was truncated at $L = 50$.

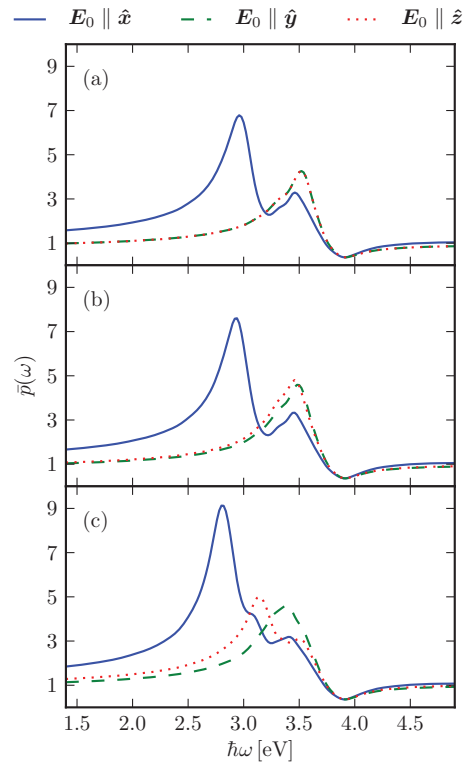

FIG. 9. (Color online) The response for an Ag dimer close to a substrate, as described by the dimensionless dipole moment of one of the spheres. As in previous cases, $d = 0.1a$, $h = 0.05a$, and $L = 50$ were used. (a) $\varepsilon_- = 1$, (b) $\varepsilon_- = 2$, (c) $\varepsilon_- = 10$.

In Fig. 9, we show the response of an Ag dimer with its axis parallel to the substrate. As previously, we have assumed $h = 0.05a$ and $d = 0.1a$. The strong interaction between the two spheres of a free-standing dimer in vacuum can be seen from Fig. 9(a) by noting the pronounced difference in response to an applied field parallel ($\boldsymbol{E}_0 \parallel \hat{\boldsymbol{x}}$) or perpendicular ($\boldsymbol{E}_0 \parallel \hat{\boldsymbol{y}}$ or $\boldsymbol{E}_0 \parallel \hat{\boldsymbol{z}}$) to the dimer axis. At least from the perspective of the dipole moment of each sphere, the influence of the substrate is not significant for $\varepsilon_- = 2$ [Fig. 9(b)], but we see substantial effects for the larger dielectric function $\varepsilon_- = 10$ [Fig. 9(c)].

While the dipole moment of the Ag spheres shows substrate effects to be weaker than those of the corresponding Drude monomer and dimer, the field-enhancement effects are still substantial. When the spheres are either close to each other and/or close to the substrate, the resonances are highly localized in space and form so-called hot spots. This is illustrated by Fig. 10, which shows the enhancement in the electric field intensity ($|\boldsymbol{E}|^2/|\boldsymbol{E}_0|^2$) for an Ag dimer. Hence, one can have local regions where the fields are strongly enhanced while their effect on the total dipole moment of the sphere is more modest.

Regarding the field enhancement in the Ag dimer, depicted in Fig. 10, we see considerable enhancement between the sphere and the substrate. This enhancement is caused by the proximity of the sphere to the dielectric substrate that creates a potential well where surface plasmons can be trapped near the south pole of the sphere. On resonance, the enhancement in the square of the field is close to 5×10^3 [Fig. 10]. If one has SERS in mind, where the cross section is enhanced by roughly the fourth power of the field, then in this case, the Raman cross section would be enhanced by 25×10^6. Thus, the influence of the dielectric substrate on the enhanced fields realized for the dimer is very substantial. Although we observed full reversal of hot-spot positions for a dimer made from Drude metal, it appears that the larger attenuation of silver $\{\mathrm{Im}[\varepsilon_j(\omega)]\}$ prohibits this phenomena in the Ag dimer. Hence, the dominant hot spot is for all frequencies of the incident light located at point 2 in the gap between the two spheres.

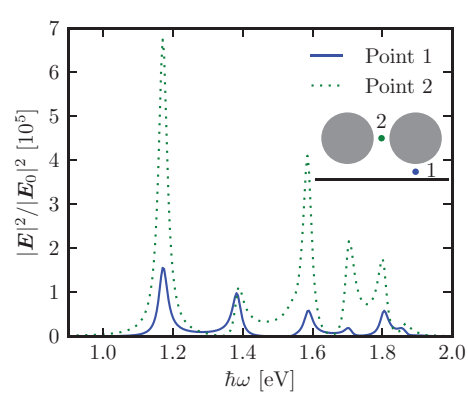

FIG. 10. (Color online) Intensity enhancement $|\boldsymbol{E}|^2/|\boldsymbol{E}_0|^2$, as a function of frequency of the applied field at points 1 and 2 for the Ag dimer on a substrate of dielectric function $\varepsilon_- = 10$. The remaining parameters are the same as in Fig. 9.

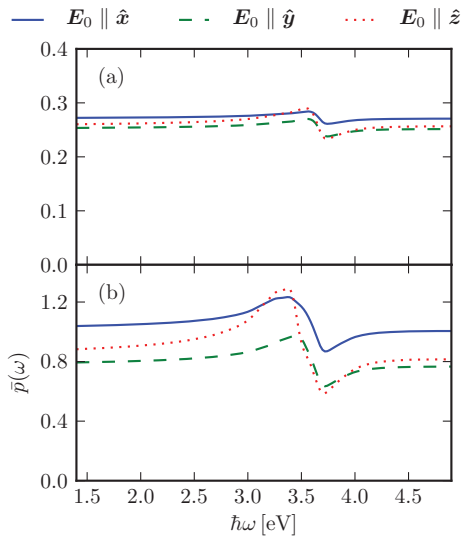

FIG. 11. (Color online) The dimensionless dipole moment of a member of a dielectric dimer placed in close proximity to an Ag surface. The dielectric functions for the two spheres forming the dimer are both (a) $\varepsilon_j = 2$ and (b) $\varepsilon_j = 10$. In both cases, we have $d = 0.1a$, $h = 0.05a$, and $L = 50$.

C. Dielectric dimer on an Ag substrate

In the literature, primary attention is directed toward nanoscale objects fabricated from plasmon-active metals. We find that dielectric particles create localized evanescent fields that stimulate the formation of localized plasmons in a nearby metallic substrate. These surface plasmons are not excited on a flat metallic surface. In this section, we consider a dielectric dimer with a frequency-independent, real, and positive dielectric function ε_j placed close to an Ag surface.

Figure 11 depicts the dimensionless dipole moment of the dielectric dimers placed very close to an Ag substrate. As before, the separation between the two spheres is $d = 0.1a$, and the height above the substrate is $h = 0.05a$. Dipole activity in the dielectric sphere is observed in the frequency range near the surface plasmon resonance of the Ag surface. Since the dielectric function of the sphere (ε_j) is frequency independent, this plasmonic activity has its origin in the Ag substrate. As expected, the effect is enhanced when the dielectric function of the spheres ε_j is increased [Fig. 11].

Figure 12 illustrates the frequency dependence of the intensity enhancement at a position between the dielectric spheres and the substrate (point 1) and between the spheres (point 2). Between the spheres (point 2), the plasmonic response of the substrate plays only a minor role in the intensity enhancement, whereas, just below the south pole of the spheres, the plasmonic activity plays a more important role, producing higher intensity enhancement for a narrow part of the spectrum. The proximity of the dielectric spheres to the substrate converts the incoming plane wave to an evanescent wave that excites surface plasmons in the Ag substrate. The consequence is that substantial intensity enhancements appear below the nanospheres near the surface plasmon frequency of the Ag surface. The physics is quite similar to the formation of a hot spot between a metal sphere and a dielectric substrate.

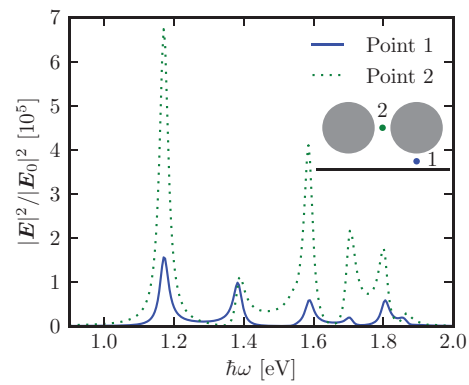

FIG. 12. (Color online) Intensity enhancements at two selected points for a dielectric dimer placed in the near vicinity of an Ag surface. The dielectric function of the spheres is $\varepsilon = 10$, and other parameters are the same as in Fig. 11.

The structure of the field enhancement near the plasmon resonance is shown in detail in Fig. 13. This figure is qualitatively similar to Fig. 7. Again, we are faced with the moving hot-spot phenomenon, since the hot spot moves from between the spheres to below the spheres as the frequency of the incident light changes.

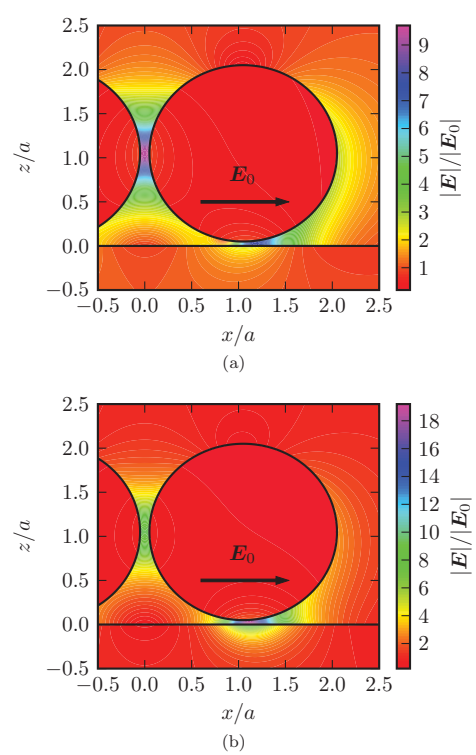

FIG. 13. (Color online) The field enhancement $|\boldsymbol{E}|/|\boldsymbol{E}_0|$ in the xz plane for a dielectric dimer above an Ag substrate. At (a) $\hbar\omega = 3.02$ eV, the highest field enhancement is found between the spheres; at (b) $\hbar\omega = 3.39$ eV, the highest field enhancement is found on the line connecting the two spheres. As shown in the figure, $\boldsymbol{E}_0 \parallel \hat{\boldsymbol{x}}$. The parameters are $\varepsilon_j = 10$, $h = 0.05a$, $d = 0.1a$, and $L = 50$.

IV. CONCLUDING REMARKS

We have formulated the theory of the interaction of nonperiodic nanosphere arrays with a substrate, and for the case of monomers and dimers, we have provided numerical studies of electric dipole moments induced by a uniform driving field and field enhancement generated by excitation of plasmon resonances. While the focus usually is placed on the interaction of metallic nanoscale objects with metallic substrates or surroundings, our emphasis has been on the interaction between metallic and dielectric materials: metallic nanoparticles on dielectric substrates or dielectric nanoparticles on metallic substrates. Such systems are, in our view, better suited for experimental examination.

For both these configurations, we find hot spots (i.e., local regions of high intensity) that are localized between the south pole of the nanosphere and the substrate. The physical origin of this behavior is an effective potential well created by the dielectric that traps and localizes plasmons in the nearby metallic component. Consider, for example, a semi-infinite slab of a model metal described by the Drude model, Eq. (5). Let the metal lie in the half space $z < 0$, and let the half space $z > 0$ be vacuum. The surface supports surface plasmons, and in electrostatic theory, these have frequency $\omega_P/\sqrt{2}$ independent of the wave vector. Instead, suppose we fill the upper half space $z > 0$ with a dielectric material whose dielectric constant is $\varepsilon_+ > 1$. This lowers the frequency of surface plasmons on the metal surface to $\omega_P(1+\varepsilon_+)^{-1/2}$. Then, if we imagine that the dielectric covers only a finite area on the metallic surface, clearly an attractive potential well is formed that can trap surface plasmons bound to the region where the dielectric is found. The frequency of these modes lies below the frequency band associated with those on the metal/vacuum interface. In our studies, we have a rather different geometry. For instance, in one configuration, we explored a dielectric sphere that is placed just a bit above the metallic substrate. The surface plasmons on the metal surface sense the presence of the dielectric through their evanescent field that extends above the metal surface. We then find plasmon modes localized in the near vicinity of the south pole of the sphere. In the case of dimers, of interest is the moving hot-spot phenomenon illustrated in Fig. 7. Small changes in excitation frequency result in a hot spot that moves from one point in the structure to another. An earlier discussion provided an example of this behavior in a rather different structure.[25]

The hot spots localized between metallic spheres and dielectric substrates and between dielectric spheres and metallic substrates, suggests that strongly enhanced nonlinear optical studies may be carried out on diverse systems, not just those where all constituents are plasmon-active metals. It would be of interest to explore field enhancements not just for spheres placed near flat substrates, but for other nanoscale objects of diverse shape as well. It should be possible to engineer structures in which large field enhancements are realized that can be exploited to study, for instance, adsorbates on insulating surfaces.

ACKNOWLEDGMENTS

We used the freely available software archive SHTOOLS authored by Mark Wieczorek (available at http://www.ipgp.fr/~wieczor/SHTOOLS/SHTOOLS.html) to evaluate the associated Legendre functions.

P.A.L. and I.S. would like to thank the Department of Physics and Astronomy, University of California at Irvine for its kind hospitality. P.A.L. would like to thank Ping Chu and Tor Nordam for interesting discussions. He would also like to thank NTH-fondet for its support of his research. The research of D.L.M. has been supported by the U. S. National Science Foundation, through Grant No. CHE-0533162. I.S. acknowledges the support from the Research Council of Norway under the program Småforsk and the NTNU Mobility program.

APPENDIX: CONSTRUCTION OF THE EQUATION SYSTEM

The expression for the electrostatic potential $\psi(\boldsymbol{r})$ is shown in Eqs. (1) and (3). This expansion is of no use before one has determined the expansion coefficients $A_{lm}^{(j)}$ and $B_{lm}^{(j)}$. To do so, we combine the series expansion of ψ and require the fulfillment of the boundary conditions at the surface of the spheres, i.e., the continuity of ψ and $\varepsilon\,\partial_n\psi$ over any interface (where $\partial_n = \hat{\boldsymbol{n}}\cdot\nabla$ denotes the normal derivative).[22] Note that the boundary conditions at the interface at $z = 0$ are already fulfilled through Eq. (4). For instance, we may consider continuity of the electrostatic potential at the surface of sphere j. This gives the condition

$$\lim_{r_j\to a_j^-}\psi_j(\boldsymbol{r}_j) = \lim_{r_j\to a_j^+}\left\{-\boldsymbol{r}\cdot\boldsymbol{E}_0 + \sum_{i=1}^{N}\psi_i(\boldsymbol{r}_i) + \sum_{i=1}^{N}\psi_{\bar{i}}(\boldsymbol{r}_i)\right\}, \quad \text{(A1)}$$

where the notation $a_j^{\pm}$ means $a_j \pm \eta$, where η is infinitesimally small and positive. For this condition to be useful, and similarly, for the equation following from the continuity of the normal components of the displacement field $\boldsymbol{D} = -\varepsilon\varepsilon_0\nabla\psi$, we need to express the potentials ψ_i and $\psi_{\bar{i}}$ for $i \neq j$ in terms of the coordinate system $\mathcal{S}_j$ centered on sphere j. One can do this by using an identity employed by Bedeaux and Vlieger.[17] This reads

$$r_i^{-l_i-1}Y_{l_i}^{m_i}(\theta_i,\phi_i) = \sum_{l_j=0}^{\infty}\sum_{m_j=-l_j}^{l_j} H(l_j,m_j,|l_i,m_i) \times \frac{Y_{l_i+l_j}^{m_i-m_j}(\theta_{ij},\phi_{ij})}{R_{ij}^{l_j+l_i+1}} r_j^{l_j}Y_{l_j}^{m_j}(\theta_j,\phi_j), \quad \text{(A2)}$$

where $\boldsymbol{R}_{ij}$ is the vector between the center of the sphere i and j, and θ_{ij} and ϕ_{ij} are the polar and azimuthal angles, respectively, which describe the direction of $\boldsymbol{R}_{ij}$. In writing Eq. (A2), we have used

$$H(l_j,m_j,|l_i,m_i) = \sqrt{4\pi}(-1)^{l_i+m_j} \times \left[\frac{2l_i+1}{(2l_j+1)(2l+1)}\right]^{1/2} \times \left[\binom{l+m}{l_i+m_i}\binom{l-m}{l_j+m_j}\right]^{1/2}, \quad \text{(A3)}$$

where $l = l_j + l_i$ and $m = m_i - m_j$. Moreover, the notation $\binom{a}{b}$ denotes the binomial coefficient. The expansion described by Eqs. (A2) and (A3) can also be applied to the image multipoles located in the substrate ($z < 0$).

We now have the electrostatic potential on each side of the surface of sphere j expressed in terms of the coordinates of system $\mathcal{S}_j$. One may generate a system of equations for the unknown amplitudes by equating the coefficients of $Y_{l_j}^{m_j}(\theta_j,\phi_j)$. When Eq. (A1) is combined with the condition that the normal components of the electric displacement field $\boldsymbol{D}$ should be continuous across the surface of sphere j, it is possible to eliminate the coefficients $B_{lm}^{(j)}$ and to generate a linear system of equations that involves only $A_{lm}^{(j)}$. When this is done, the following linear system of equations results:

$$\begin{aligned}-b_{1m_j}\delta_{1,l_j} = & A_{l_jm_j}^{(j)}\frac{l_j\varepsilon_j + \varepsilon_+(l_j+1)}{l_j(\varepsilon_j - \varepsilon_+)}a_j^{-2l_j-1} \\ & - \sum_{l_j,m_j} A_{l_im_i}^{(j)} H(l_j,m_j|l_i,m_i)\frac{Y_{l_i+l_j}^{m_i-m_j}(\theta_{ij},\phi_{ij})}{R_{ij}^{l_j+l_i+1}} \\ & + \sum_{i\neq j}\sum_{l_i,m_i} A_{l_im_i}^{(i)} H(l_j,m_j|l_i,m_i)\left[\frac{Y_{l_i+l_j}^{m_i-m_j}(\theta_{ij},\phi_{ij})}{R_{ij}^{l_j+l_i+1}}\right. \\ & \left. + (-1)^{l_i+m_i}\beta\frac{Y_{l_i+l_j}^{m_i-m_j}(\theta_{\bar{i}j},\phi_{\bar{i}j})}{R_{\bar{i}j}^{l_j+l_i+1}}\right], \end{aligned} \tag{A4}$$

where $\beta = (\varepsilon_+ - \varepsilon_-)/(\varepsilon_+ + \varepsilon_-)$ and $l_j = 1,2,3,\ldots,L$ and $m_j = 0, \pm 1, \pm 2, \ldots, \pm l_j$. The coefficients b_{lm} are the expansion coefficients of the applied field $\boldsymbol{E}_0$ in terms of the spherical harmonics. The nonzero b_{lm} coefficients (in the case of uniform $\boldsymbol{E}_0$) are given by[17,19]

$$b_{10} = -E_0\sqrt{\frac{4\pi}{3}}\cos\theta_0, \tag{A5a}$$

$$b_{1\pm1} = \pm E_0\sqrt{\frac{2\pi}{3}}\sin\theta_0 e^{\mp i\phi_0}, \tag{A5b}$$

where θ_0 is the angle between the external field and the positive z axis and ϕ_0 is the azimuthal angle that describes the angle between the projection of the external field onto the xy plane and the positive x axis. As the Laplace equation is linear, we only need to solve for three different directions of $\boldsymbol{E}_0$ ($\boldsymbol{E}_0$ parallel to $\hat{\boldsymbol{x}}$, $\hat{\boldsymbol{y}}$, and $\hat{\boldsymbol{z}}$). The response to an applied field pointing in any other direction can be constructed through superposition of these three cases.

Equation (A4) gives us $N(L+1)^2 - 1$ linear equations in the expansion coefficients $A_{lm}^{(j)}$, and we have $N(L+1)^2$ unknowns. The final equation results from the continuity of the normal component of $\boldsymbol{D}$ at the spherical interfaces. Taking the normal (i.e., radial) derivative of the B_{00} term, we see that this term vanishes $[\partial_{r_j} B_{00}\, Y_0^0(\theta_j,\phi_j) = 0]$. This means that $A_{00} = 0$, related to the fact that the nanoparticles are assumed to carry no charge. Hence, the equation system is closed, and we can expect to find a unique solution.

Finally, the resonances for an isolated sphere in a homogeneous background of dielectric function ε_+ can be obtained from Eq. (A4). By neglecting all contributions from other particles and image multipoles, i.e., to keep only the first term on the right-hand side of Eq. (A4), one is essentially left with the isolated sphere case. Under this assumption, the resulting equation can readily be solved to give

$$A_{lm} \propto \frac{1}{l\varepsilon + \varepsilon_+(l+1)},$$

where ε is the dielectric function of the sphere. Hence, the resonance positions are determined by the zeros of the real part of the denominator of A_{lm}:

$$\mathrm{Re}\,[l\varepsilon + \varepsilon_+(l+1)] = 0.$$

If we assume for ε the Drude model with $\gamma = 0$ ($\varepsilon = 1 - \omega_P^2/\omega^2$), which in our case, is a good approximation, we get the following resonance frequencies for the isolated sphere:

$$\omega_l = \omega_P\sqrt{\frac{l}{2l+1}}.$$

For systems containing more than a single isolated sphere, such as the ones discussed in this paper, these resonance frequencies are typically modified due to particle-particle or particle-substrate interactions.

*paul.anton.letnes@gmail.com

[1] M. Moskovits, Rev. Mod. Phys. **57**, 783 (1985).
[2] S. Nie and S. R. Emory, Science **275**, 1102 (1997).
[3] J. Jiang, K. Bosnick, M. Maillard, and L. Brus, J. Phys. Chem. B **107**, 9964 (2003).
[4] D. S. Chemla, J. P. Heritage, P. F. Liao, and E. D. Isaacs, Phys. Rev. B **27**, 4553 (1983).
[5] T. Ichimura, N. Hayazawa, Y. Inouye, and S. Kawata, J. Raman Spectrosc. **34**, 651 (2003).
[6] D. R. Fredkin and I. D. Mayergoyz, Phys. Rev. Lett. **91**, 253902 (2003).
[7] I. D. Mayergoyz, D. R. Fredkin, and Z. Zhang, Phys. Rev. B **72**, 155412 (2005).
[8] S. Zou and G. C. Schatz, Nanotechnology **17**, 2813 (2006).
[9] R. Arias and D. L. Mills, Phys. Rev. B **68**, 245420 (2003).
[10] G. Bachelier, I. Russier-Antoine, E. Benichou, C. Jonin, N. Del Fatti, F. Vallée, and P.-F. Brevet, Phys. Rev. Lett. **101**, 197401 (2008).
[11] J. M. Gérardy and M. Ausloos, Phys. Rev. B **22**, 4950 (1980).
[12] T. Yamaguchi, S. Yoshida, and A. Kinbara, Thin Solid Films **21**, 173 (1974).
[13] R. Ruppin, Surf. Sci. **127**, 108 (1983).
[14] C. E. Román-Velázquez, C. Noguez, and R. G. Barrera, Phys. Rev. B **61**, 10427 (2000).
[15] C. Noguez, J. Phys. Chem. C **111**, 3806 (2007).
[16] S. Y. Lee, L. Hung, G. S. Lang, J. E. Cornett, I. D. Mayergoyz, and O. Rabin, ACS Nano **4**, 5763 (2010).
[17] D. Bedeaux and J. Vlieger, *Optical Properties of Surfaces* (Imperial College Press, London, 2004).

[18]R. Lazzari, I. Simonsen, and J. Jupille, Europhys. Lett. **61**, 541 (2003).
[19]I. Simonsen, R. Lazzari, J. Jupille, and S. Roux, Phys. Rev. B **61**, 7722 (2000).
[20]R. Lazzari, S. Roux, I. Simonsen, J. Jupille, D. Bedeaux, and J. Vlieger, Phys. Rev. B **65**, 235424 (2002).
[21]R. Lazzari and I. Simonsen, Thin Solid Films **419**, 124 (2002).
[22]J. D. Jackson, *Classical Electrodynamics*, 3rd ed. (Wiley, New York, 1999).
[23]P. Chu and D. L. Mills, Phys. Rev. Lett. **99**, 127401 (2007).
[24]P. Chu and D. L. Mills, Phys. Rev. B **77**, 045416 (2008).
[25]P. A. Letnes and I. Simonsen, Phys. Status Solidi B **247**, 2084 (2010).
[26]H. Tamaru, H. Kuwata, H. T. Miyazaki, and K. Miyano, Appl. Phys. Lett. **80**, 1826 (2002).
[27]Note that we do not plot the square of $|\boldsymbol{E}|/|\boldsymbol{E}_0|$, as the enhancement then becomes very large, in which case, it is difficult to synthesize a nicely color-coded figure.